4 Tbit/s transmission reach enhancement using 10x400 Gbit/s super-channels and polarization insensitive dual band optical phase conjugation

A. D. Ellis[1]*, M. Tan[1], M. A. Iqbal[1], M. A. Z. Al Khateeb[1], V. Gordienko[1], G. Saavedra. M.[2], S. Fabbri[1], M. F. C. Stephens[1], M. E. McCarthy[1], A. Perentos[1], I. D. Phillips[1], D. Lavery[2], G. Liga[2], R. Maher[2], P. Harper[1], N. J. Doran[1], S. K. Turitsyn[1], S. Sygletos[1], P. Bayvel[2]

(*Invited paper*)

***Abstract*—In this paper, we experimentally demonstrate the benefit of polarization insensitive dual-band optical phase conjugation for up to ten 400Gbit/s optical super-channels using a Raman amplified transmission link with a realistic span length of 75km. We demonstrate that the resultant increase in transmission distance may be predicted analytically if the detrimental impacts of power asymmetry and polarization mode dispersion are taken into account.**

***Index Terms* — Fiber nonlinear optics, Channel models, Optical fiber communication, Optical signal processing.**

I. Introduction

In order to maximize the capacity of single mode fiber based optical communication systems it is necessary to simultaneously minimize amplified spontaneous emission using distributed amplification [1], maximize spectral efficiency using super-channels [2] and fully compensate for all deterministic nonlinear impairments [3]. Whilst Raman amplification and super-channels are becoming increasingly commercially available, the optimum means to compensate nonlinearity is the focus of much research. Perhaps the earliest proposal to compensate simultaneously for dispersion [4] and nonlinearity [5] was to use optical phase conjugation (OPC) at the midpoint of the link. Initial studies focused on on-off keyed modulation in optically amplified link [6-9]. OPC was also combined with other forms of mitigating nonlinearity, such as soliton transmission, and suggested that the interaction between signal and noise (expressed as Gordon-Haus jitter for solitons) could also be partially compensated [9]. Preliminary studies on OPC included the compensation of nonlinearity for high speed TDM channels [6], WDM channels [7] and even addressed installation issues [8] and operation over field installed fibers [10]. However, in common with coherent detection, simpler alternative technological advances such as dispersion management and forward error correction reduced the market need for OPC. Commercial imperatives, coupled with technological capability to deliver solutions, have seen amplifier spacing increase to the region of 80-100 km. The introduction of transmitter digital signal processing [11] and digital coherent receivers [12] have also resulted in further subtle changes to system design. Our current understanding of nonlinear propagation for high spectral efficiency systems [13-15] with tight channel spacing implies there is no longer a tradeoff between high local dispersion, to minimize nonlinearity from other co-propagating WDM channels (inter-channel), and low path-average dispersion, to minimize nonlinear distortion within a channel (intra-channel).

As information spectral densities rise above 8 b/s/Hz (polarization multiplexed 16QAM) there is renewed interest in the compensation of nonlinearities. Candidate technologies include single channel [16] and wide-bandwidth digital back propagation [17], phase conjugate coding [18], pre-compensation [19] and renewed interest in in-line OPC [20-32]. We have recently shown that of these alternatives, ideal in-line OPC uniquely offers disruption of parametric noise amplification [20] and thus overcomes the nonlinear Shannon limit [15]. Assuming certain symmetry conditions are satisfied, an ideal OPC provides compensation of both intra-channel and inter-channel nonlinear effects. One notable advantage of OPC is that all channels are compensated in a single device. This offers the prospect of energy savings when compared to per channel (or per-super-channel [17]) digital approaches. Impressive performance enhancements for WDM systems have been reported where reasonable transmission symmetry in power [21-23] and dispersion [24] been implemented. Even greater performance benefits are predicted for systems employing more than one OPC [20-21, 24-25]. As we approach the fundamental limits of single mode optical fibers, new opportunities for OPC technologies become clear and experiments over field installed fibers have renewed

Manuscript received September 01, 2015. Authors indicated with the superscript 1 are with Aston Institute of Photonic Technologies, Aston University, Aston Triangle, Birmingham, B4 7ET, UK (corresponding author phone: +44(0)121 204 3075; e-mail: andrew.ellis@aston.ac.uk). Authors indicated with the superscript 2 are with Optical Networks Group, University College London, Torrington Place, London, WC1E 7JE, UK.

progress [26,27], along with experiments using the necessary high information spectral density channels [23, 28-30].

We recently reported the first combination of polarization multiplexed 16QAM optical super-channels, lossless Raman amplification and dual-band optical phase conjugation [32], with a reach in excess of 2,700 km for multiple 400 Gbit/s Nyquist super-channels with a record total bit rate of 2.4 Tbit/s. In this paper we extend these results, providing more details of the experimental configuration and the analytical model used to accurately predict the system performance. We additionally provide details on the performance of the system for different numbers of super-channels, up to a maximum capacity of 4 Tbit/s. We report significant reach enhancements, even in the presence of polarization mode dispersion (PMD) and link asymmetry, confirming the potential of OPC to overcome the non-linear Shannon limit.

The remainder of the paper is organized as follows. The system model is described in Section II, where we introduce an additional term to the conventional model to account for parametric noise amplification and estimate the impact of PMD and power symmetry. Section III introduces our experimental configuration, including the transmitter, the loop configuration and the OPC design. In Section IV the system performances are presented and compared to theoretical predictions, whilst Section V concludes the paper.

II. Theoretical Performance

Several analytical models for nonlinear transmission performance have been proposed recently [13-15] which accurately account for inter-channel nonlinear interactions. However, these models suggest that if inter-channel nonlinearity is fully compensated the system performance reverts to the conventional Shannon limit and is essentially unbounded [34]. In considering the performance of a nonlinearity compensated system, it is necessary to consider the efficiency of the nonlinear compensation, and the nonlinear interactions associated with the co-propagating amplified spontaneous emission noise. We thus consider a generalized format for the nonlinear Shannon limit, quantifying the maximum possible nonlinear compensation and considering the interaction between the signal and amplified spontaneous emission (parametric noise amplification), but neglecting signal depletion [35] effects and other noise dependent terms (nonlinear phase noise [36] and nonlinear noise). The nonlinear signal to noise ratio is then given by [20, 37, 38]:

$$SNR_{NL} \approx \frac{P_S}{NP_N + N_{OPC}P_O + N\eta\left(1-\eta_S\eta_P\right)P_S^3 + 3f_{SN}\eta P_N P_S^2} \quad (1)$$

where P_S represents the signal power spectral density, N the number of spans, P_N the amplified spontaneous emission power spectral density generated by each span, P_o the additional amplified spontaneous emission power spectral density generated by the OPC, N_{OPC} the number of OPC devices, η a coefficient of nonlinearity depending approximately logarithmically on the WDM signal bandwidth B_S (which should take into account spectral broadening during transmission [33]), η_P represents the reduction in the efficiency of nonlinear compensation (NLC) due to the limited effective bandwidth of the nonlinear compensation system PMD, η_S the reduction due to imperfect power symmetry. In equation 1, the first term in the denominator represents accumulated amplified spontaneous emission, the second term additional noise associated with the OPC device, the third term represents the residual nonlinearity (scales with P_S^3), and the final term parametric noise amplification (scales with P_S^2). With ideal compensation ($\eta_P\eta_S=1$), parametric noise amplification becomes the most significant limiting source of nonlinear noise [3]. Since the noise from each span is amplified by all remaining spans, it scales nonlinearly with length in a manner given by [20];

$$f_{SN}(N) \approx \left(\frac{N}{N_L} + N_L \sum_{n=1}^{\frac{N}{N_L}-1} n \right) \quad (2)$$

where $N_L=N_{OPC}+1$ represents the number of segments, N_L =1 for digital signal processing, 2 for a single OPC (mid-link). Eqn. 2 assumes uniformly spaced OPCs. To significantly simplify the calculation, we heuristically model the impact of PMD by assuming that only the spectrum which would pass a Lyot filter with the mean birefringence of the link may meaningfully contribute to the compensation of nonlinearity. This approximation is in close agreement with recently reported detailed models for the impact of PMD [38]. Our heuristic model gives [37];

$$\eta_P \approx \frac{Ci\left(Min(B_C\sqrt{L}\sigma_P, \pi/2)\right) - Ci\left(f_W\sqrt{L}\sigma_P\right)}{Log(B_s/f_W)} \quad (3)$$

where B_C is the effective bandwidth of the NLC (approximately equal to the bandwidth of the coherent receiver provided $B_C>>f_W$), L the total compensated length, σ_P the PMD parameter, f_W the nonlinear phase matching bandwidth [13,38], and Ci the Cosine Integral. Extending the calculation of asymmetry for a single span reported in [21] to a multi-span system, the asymmetry parameter η_S is given by;

$$\eta_S = 1 - \frac{\int_0^{NL/N_L} \left| P_S(z) - P_S(N.L/N_L - z) \right| .dz}{\int_0^{NL/N_L} P_S(z).dz} \quad (4)$$

To quantify the detrimental impact of PMD and power asymmetry, we consider the reach of a typical 16-QAM super-channel based transmission system using an OPC.

Figure 1a shows the theoretical reach of a 16QAM Nyquist WDM system without nonlinearity compensation (blue) and with an ideal midpoint OPC (red). The reach is defined as the largest number of spans for which Eqn. 1 predicts a signal to noise ratio of over 10.5 dB (corresponding to a pre FEC BER of 10^{-3}). We have assumed a span length (pump spacing) of 80 km, a nonlinear coefficient of 1.2 $W^{-1}km^{-1}$, a dispersion coefficient of 17 ps/nm/km, and an equivalent Raman noise

coefficient of 1.755. Without nonlinearity compensation, the reach of this system naturally declines with increasing signal bandwidth from 5,400 km for a single super-channel with 100 GHz bandwidth to 4,000 km for the full C band (5 THz). The reduction in reach with system bandwidth is modest since beyond the fiber phase matching bandwidth ($f_W \approx 4$ GHz) the bandwidth dependence of η is approximately logarithmic. An approximately constant reach enhancement factor of 4.7 is observed when an OPC is added. For ideal compensation if we compare a system with ideal OPC to a system with zero parametrically amplified noise Eqn. 1 predicts a constant reach enhancement of a factor $1.17\ SNR^{1/3}$. Including parametric noise amplification in the uncompensated case further increases the reach enhancement. Note that for all practical received SNRs the reach enhancement for an OPC based system exceeds the factor of two reach enhancement expected from the use of mid-point regenerators.

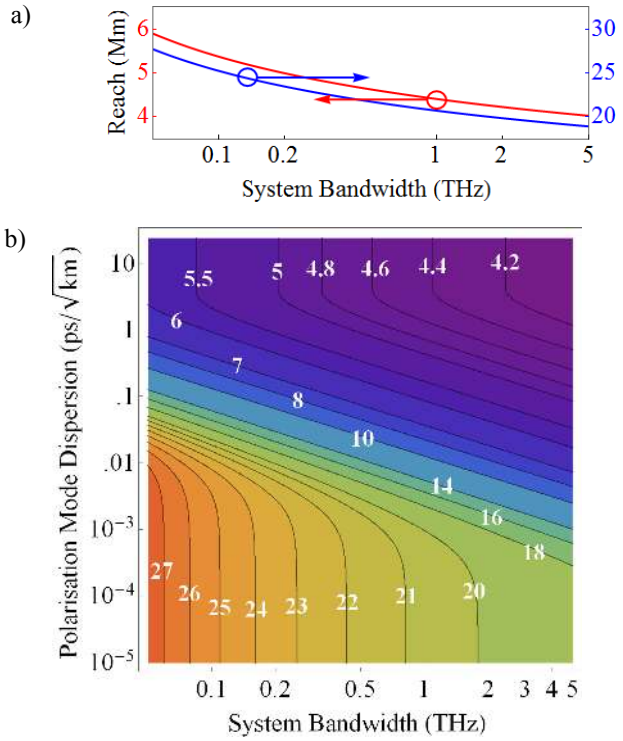

Fig. 1: (a) Variation in reach with (blue) and without (red) ideal nonlinearity compensation for a 16 QAM Nyquist WDM system. (b). Variation in reach (in Mm) of a 16QAM Nyquist WDM system with ideal nonlinearity compensation, a single midpoint OPC, and ideal power symmetry, plotted as a function of polarization mode dispersion and total signal bandwidth.

Figure 1b shows data calculated in the same way as a function of PMD parameter and overall signal bandwidth with a single OPC and ideal power symmetry (calculated using Eqns. 1-3). Contour values along the top x-axis (very high PMD) are equivalent to the uncompensated curves in Fig 1a, whilst those along the lower x-axis (negligible PDM) correspond to ideal compensation (also shown in Fig. 1a). Including an OPC dramatically increases the reach for low bandwidth signals from around 5,000km (Fig 1a), since the impact of PMD is small, and full compensation of nonlinearity may be achieved. However, with a PMD coefficient of 0.1 ps/√km, a signal of 120 GHz bandwidth would only see its reach doubled from 5,500 km to 11,000km due to the reduction in the effectiveness of nonlinear compensation. Using spun fiber with PMD coefficient below 0.04 ps/√km enables the bandwidth where reach is doubled to be increased to 375 GHz. These dramatic reductions in compensation efficiency are due to the stochastic polarization walk-off between widely spaced channels which renders simple forms of nonlinearity compensation ineffective.

Power symmetry further degrades the expected reach enhancement as shown in Figure 2 for a symmetry factor η_S of 82%. Reach enhancement is significantly capped as power asymmetry is introduced, and even for 0.1 ps/√km PMD, signal bandwidths above 400 GHz are required before polarization walk-off dominates the performance degradation. However, for conventional fibers and signal bandwidths in the region of a THz, both power asymmetry and PMD are important restrictions of the effectiveness of OPC based nonlinearity compensation, and will be considered in the analysis of the experimental results.

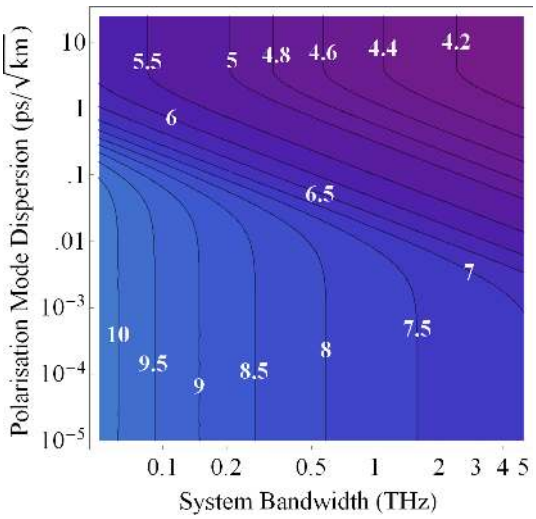

Fig.2. Variation in reach (in Mm) of a 16QAM Nyquist WDM system with ideal nonlinearity compensation, a single midpoint OPC, and power asymmetry of 82%, plotted as a function of PMD and total signal bandwidth.

III. Experiment

In this section, we detail the experimental configuration including the 400 Gbit/s Nyquist WDM super-channel transmitter (Fig. 3); the Raman laser based recirculating loop configuration (Fig. 4), and the dual band OPC (Fig. 6). For WDM transmission, a combination of DFB, external cavity and fiber lasers formed two bands of up to 5 lasers each centered at 193 and 194.6 THz with 100 GHz spacings. There was no observable difference in performance between fiber lasers and external cavity lasers, confirming that degradations due to linewidth and frequency instability were low. For each measurement the DFB lasers for a particular super-channel under test was replaced in turn with a tunable external cavity laser. The 10 independent lasers were multiplexed together and subsequently modulated with Nyquist shaped 10Gbaud (2 samples per symbol) 16QAM in-phase (I) and quadrature (Q)

electrical signals (with 2^{15} pseudo random bit sequences) using an IQ modulator. The symbol rate was restricted by the available equipment; we expect similar results for single carrier solutions. The digital Nyquist filter had a roll off factor of 0.01 at the output of the arbitrary waveform generator. The resulting optical Nyquist signals were amplified and passed into an optical comb generator. This consisted of two stages, The first stage was a Mach Zehnder modulator (MZM) driven at 20.2 GHz and biased to provide a 3 line comb. These 20.2 GHz spaced signals were split in the second stage and one copy was frequency shifted by 10.1 GHz using a single side band modulation scheme with over 30 dB extinction ratio. The other copy was delayed by 5 symbols before recombining to form a super-channel with a spectral width of approximately 60 GHz. After amplification, the signals were polarization multiplexed with a 20.48 ns relative delay. The gross data rate for a super-channel was 480 Gbit/s, which equates to a net data rate of 400 Gbit/s assuming 20% overhead for FEC [40].

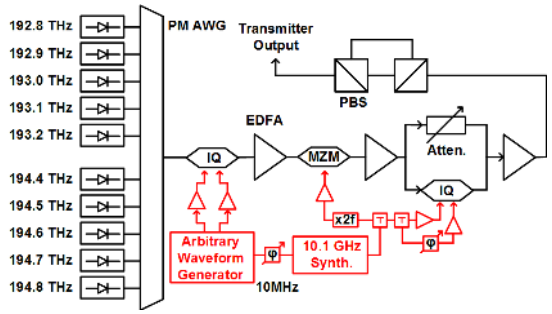

Fig. 3. Transmitter configuration showing signal lasers (diode signs) polarization maintaining arrayed waveguide grating (PM AWG) nested (IQ) and conventional (MZM) modulators, amplifiers (triangles), polarization beam splitters (PBS), frequency doubler (x2f) and phase shifters (φ).

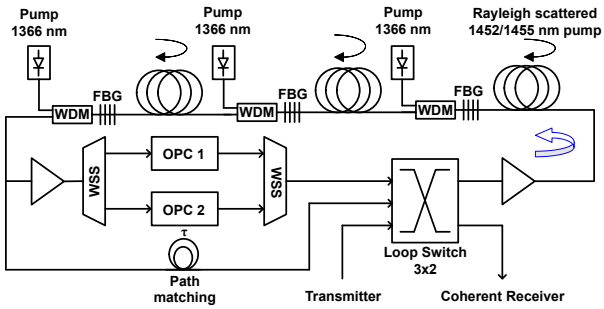

Fig. 4. Schematic diagram of recirculating loop showing; second order Raman amplified link and dual band OPC and loop configuration (1366nm pump, 1452/1455nm FBG), showing wavelength selective switches (WSS), optical phase conjugators (OPC), wavelength division multiplexers (WDM) and transmission fiber (loops) and other components defined in Fig. 3.

The signals were launched into a multi-path recirculating loop via an erbium doped fiber amplifier and passed through three Raman laser based spans. In each of the 75 km Sterlite OH-LITE™(E) fiber spans, the 1452/1455 nm pump (the spread of wavelengths enhancing the gain flatness) was generated by lasing in a cavity formed by a fiber Bragg grating (FBG) at the fiber output, and distributed Rayleigh scattering throughout the link, pumped by a 1366 nm fiber laser with 1.1 W launched power in each span [39]. The equivalent 2nd order Raman amplifier configuration gave a near symmetric power profile to maximize the efficiency of OPC-based nonlinearity compensation as illustrated in Fig 5. This shows an optical time domain reflectometer measurement of the second span plotted both forwards and backwards. The same data is duplicated to illustrate the impact of the WDM coupler losses. A 6 dB power excursion and a power asymmetry of only 18% (or symmetry of 82%) is observed over the 3 x 75 km link. Since each individual span has asymmetry of less than 8%, the majority of the asymmetry is attributed to the finite loss of the pump couplers and fiber Bragg gratings (0.5 dB per span).

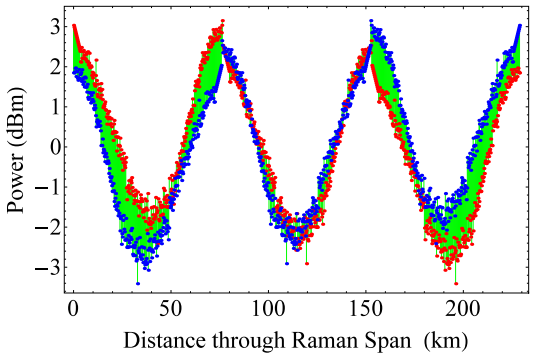

Fig. 5: Signal power evolution through one span (red) and with direction reversed (blue). The trace from a one span repeated every 75km with 0.5dB loss artificially added for illustration. Asymmetry highlighted in green.

The signals propagated through this link a number of times (which included a gain flattening filter and an amplifier to overcome loop specific losses), before entering the dual OPC (Fig. 6). Here the two bands of between one and five 400 Gbit/s super-channels were amplified, split into two parallel paths using a wavelength selective switch (WSS), giving ~12 dBm total power per band, and conjugated in two nearly identical single pump polarization-diverse OPCs [41]. The OPCs used independent pump lasers (external cavity lasers, specified with 100 kHz linewidth) and aluminum doped highly-nonlinear fibers with lengths, fiber loss and nonlinear coefficients of 100 m, 6.3 dB/km and 6.9 /(W.km) respectively. At the output of each OPC, the residual pumps were blocked using thin-film notch filters and the conjugated bands gain-equalized and combined using a second WSS.

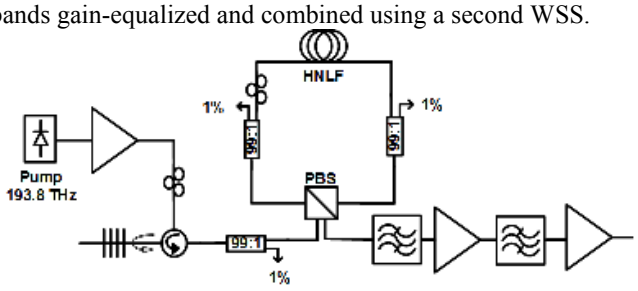

Fig. 6. Schematic diagram of one OPC showing pump laser optical amplifiers, polarization controllers (three loops), fiber grating (four vertical lines), circulator (circle enclosing curved arrow) tap couplers (boxes including ratio), PBS, highly nonlinear fiber (HNLF) and bulk grating based optical filters (boxes with wavy lines) and other components defined in Fig. 2 and Fig. 3.

Importantly, unlike previous experiments this ensured that all channels were launched simultaneously, and that intra-band nonlinearity compensation was performed on both bands

simultaneously. After propagating through the Raman spans for an identical number of recirculations, a portion of the super-channel under test was filtered using a 20 GHz optical filter, detected using a conventional coherent receiver with 25 GHz analogue bandwidth and processed using digital signal processing code optimized for Nyquist signals [42].

IV. Experimental Results

In order to establish the basic potential of OPC to enhance transmission reach we consider initially the transmission of two optical super-channels, one in each band (at 193 and 194.6 THz). We then increased the spectral width of the system by adding super-channels to each band. For each experiment we initially optimized the signal launch power at a transmission distance of 1350 km. We averaged the BER of the central sub-channel of the central super-channel of each band. Example results are shown in Fig. 7 for the case of two and ten super-channels (additional data is available see link in the footnote to page 1). Similar nonlinear thresholds of +1 dBm without and +3 dBm with OPC are observed for both configurations.

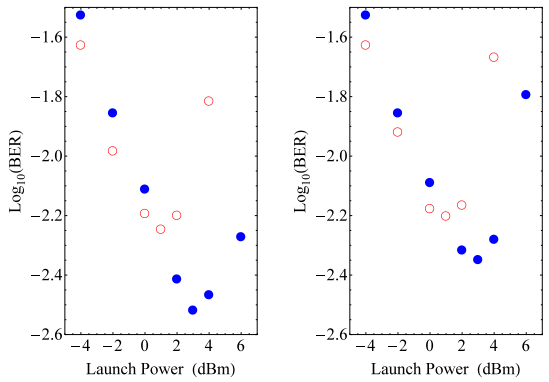

Fig. 7: Performance with the BER averaged over central channels of the central super-channels of both the upper and the lower bands with (blue) and without (red) OPC as a function of power for two (left) and ten (right) super-channels measured at a transmission distance of 1350km.

For each configuration we then measured the performance as a function of transmission distance at the optimum launch power. The spectra at transmission distances of 3,600 km and 2,250 km with and without OPC respectively along with the BER results are shown in Fig. 8 for the case of two super-channels, and in Fig. 9 for the case of 10 super-channels. The high quality of the super-channel generation and the amplitude of the unwanted sidebands (more than 20 dB suppressed) can be seen clearly in the spectra. BER measurements averaged over the central channels of each band are plotted. For two super-channels (Fig. 8) a reach enhancement of approximately 60% was observed, which remains somewhat less than the theoretical predictions (eg Fig. 2). We believe that this is due to the additional OSNR penalty associated with the insertion of the OPC device (second term in the denominator of Eqn. 1, omitted from Fig.1 and Fig.2). The nonlinear compensation calculations only allowed for compensation of one band of signals (since the second band was neither time nor polarization aligned in the dual path OPC) and the resultant signal to noise ratios were converted to BER assuming Gaussian noise distributions and Gray mapping. The curve fits correspond to a Raman noise power spectral density of 10-20 W/(km.Hz) and 0.1 ps/√km PMD. The effective nonlinear coefficient integrated over the signal spectrum (η) and the transmitter SNR varied with the number of super-channels. For one (five) super-channel(s) per band these coefficients were 20 (16.5) dB and 0.20 (0.22) $THz^2/(W^2.km)$ respectively. All other parameters were measured from the experimental set up. An excellent agreement may be observed between analytical predictions (solid lines) and experimental measurements (dots) when OPC loss and transmitter OSNR are taken into account.

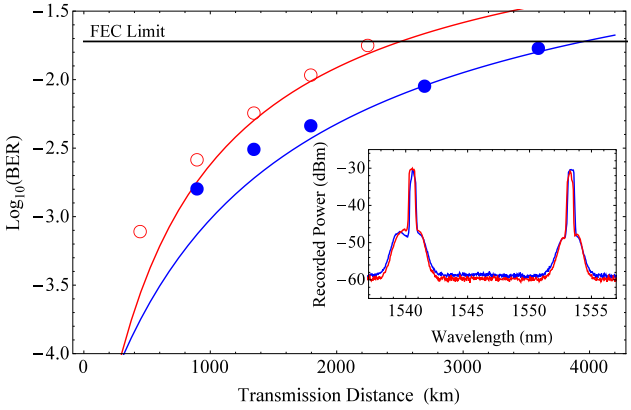

Fig. 8: Measured (dots) and calculated (lines) performance of the central channel of the higher frequency band (without OPC, lower frequency band with OPC) with (blue) and without (red) OPC for two super-channels versus transmission distance. Inset: Spectra after 3600km transmission with (blue) and 2250km without (red) OPC.

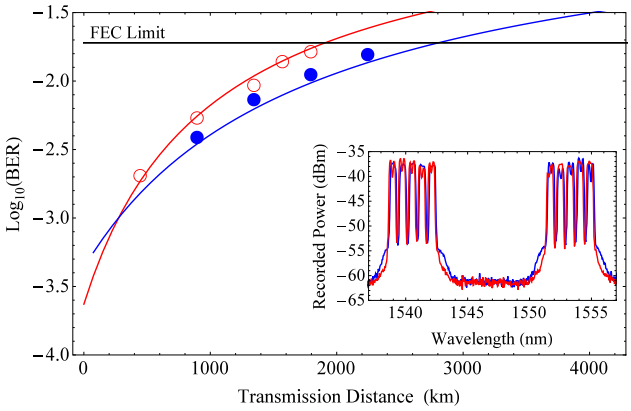

Fig. 9: Measured (dots) and calculated (lines) performance of the central channel of the higher frequency band (without OPC, lower frequency band with OPC) with (blue) and without (red) OPC for ten super-channels versus transmission distance. Inset: Spectra after 1,800 km transmission with (blue) and 1,575 km without (red) OPC.

The transmission performance of the system when propagating six super-channels (2.4 Tbit/s total, 6 super-channels) was reported in [32], where the optimum launch powers were 4 dBm with OPC and 1 dBm without. The reach enhancement reported in [32] was approximately 55%. Figure 9 shows the BER performance as a function of transmission distance for five super-channels per band (4 Tbit/s total capacity). Again excellent agreement between theory and experiment is observed, although the impact of polarization

mode dispersion over the increased bandwidth has reduced the reach enhancement to less than 20%.

The dependence of reach enhancement on the system configuration is illustrated in Figures 10 and 11. In Figure 10 we plot the reach where all super-channels (rather than just the central super-channel shown in Figures 8 and 9) exhibit a pre FEC BER of $\leq 1.9 \times 10^{-2}$ both with and without dual band OPC (central sub-channel in each super-channel of the band measured). Theoretical performance with OPC degraded by power symmetry is shown by the blue dashed curve, degraded by PMD and power symmetry by the blue curve and without OPC by the red curve. Both theoretical curves include an estimation of the OSNR impact of inserting the OPC. The experimental results are represented by the dots with single sided error bars representing the minimum transmission distance step size in the recirculating loop (450 km with OPC and 225 km without). This method of plotting the results clearly shows that the theoretically predicted transmission reach always falls between the experimentally measured reach (last recirculation below the FEC threshold) and the next recirculation. Theoretically the reach decreases with increasing number of super-channels since the nonlinear threshold decreases and depends on the signal to noise ratio without OPC [20]. For an ideal OPC, the maximum reach should exceed 7,500 km, but if only the nonlinearity of one band is compensated; this reduces to 5,000 km. As predicted by Figures 1 and 2, the observed power fluctuation between spans (0.5dB in this case) further degrades the performance to less than 4,000 km (dashed line). PMD reduces the reach by a further 300 km (solid line).

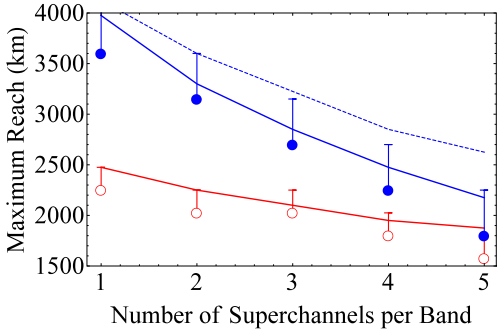

Fig. 10: Measured (dots) and calculated reach with (blue) and without (red) OPC. Error bars reflect the length of each loop circulation. Solid lines represent calculated performance with PMD and power asymmetry taken into account; dashed line only includes power asymmetry.

Figure 11 illustrates the BER performance of each super-channel at the maximum reach reported in Fig. 10, with all but one of the super-channels operating below the assumed FEC limit, allocating all of the overhead to error correction. For system configurations employing a small number of super-channels we observe broadly similar BER performance for all super-channels. However, for the eight and ten super-channel systems some variation in performance is observed, with edge channels degraded slightly. For the innermost channels of each band this is believed to be caused by the spectral filters employed to enable dual band operation. For the outermost conjugated channels (showing higher degradation) this is believed to be due to the frequency dependence of the OPC conversion efficiency, whilst we attribute the difference between the bands to slight gain and noise figure tilts in our Raman amplifiers [43].

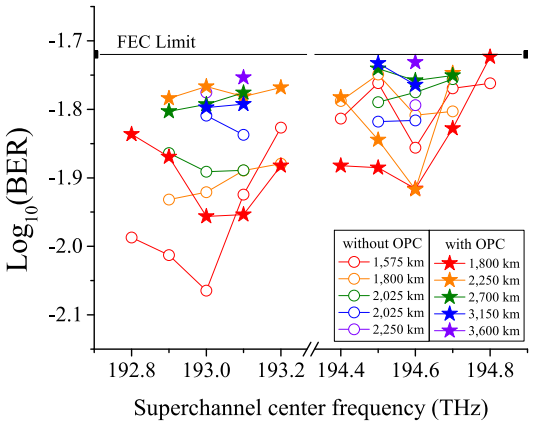

Fig. 11: Measured performance at maximum measured reach of central channel of each super-channel following transmission without nonlinearity compensation (open symbols) and with compensation of nonlinearity using an OPC (closed symbols) for ten (red) eight (orange), six (green) four (blue) and two (purple) super-channels. Transmission reaches recorded in the legend.

V. Conclusions

In this paper we have demonstrated, for the first time, dual band optical phase conjugation of an optical super-channel using 75 km spans of standard single mode fiber. We are able to substantially eliminate deterministic nonlinear penalties. This nonlinearity compensation allows a 60% increase in reach for two simultaneously transmitted 400 Gbit/s 16QAM super-channels, falling to a reach enhancement of 20% for ten simultaneously transmitted super-channels. This represents a record bit rate-distance product for an optical phase conjugation based system (8Mm.Tbit/s). These experimental results have been used to verify simple analytical models of OPC performance in the presence of degradations due to power symmetry and PMD. Despite these penalties, we observe significant reach enhancement from OPC.

Acknowledgment

This work was partially supported by the ECs 7th Framework Program under grant number 318415 (FOX-C), the EPSRC projects EP/J017582/1, EP/L000091/1 & EP/J009709/1 (UNLOC, PEACE and FOPA respectively), the Marie Curie Action grant number 608099 (ICONE), and The Royal Society (WM120035-TEST). The authors thank Sterlite Technologies and Finisar for their support.

References

[1] A. Carena, V. Curri, and P. Poggiolini,"On the Optimisation of Hybrid Raman/Erbium-Doped Fiber Amplifiers," *IEEE Photonics Technol. Lett.,* vol. 13, no. 11, pp.1170-1172, Nov 2001.

[2] D. Qian, et al.," 101.7-Tb/s (370×294-Gb/s) PDM-128QAM-OFDM Transmission over 3×55-km SSMF using Pilot-based Phase Noise Mitigation," in *Proc. Optical Fiber Communication Conference*, Anaheim, California, 2011, paper PDPB5.

[3] D. Rafique and A.D. Ellis, "Impact of signal-ASE four-wave mixing on the effectiveness of digital back-propagation in 112 Gb/s PM-QPSK systems," *Optics Express*, vol. 19, no.4, pp. 3449-3454, Feb 2011.

[4] D.M. Pepper, and A. Yariv, "Compensation for phase distortions in nonlinear media by phase conjugation," *Optics Lett.,* vol. 5, no. 2, pp. 59-60, Feb 1980.

[5] R.A. Fisher, B.R. Suydam, and A. Yariv, "Optical phase conjugation for time-domain undoing of dispersion self-phase modulation effects," *Optics Lett.*, vol. 8, no. 12, pp. 611-613, Dec 1983.

[6] D.D. Marcenac, et al., "40 Gbit/s transmission over 406 km of NDSF using mid-span spectral inversion by four-wave-mixing in a 2 mm long semiconductor optical amplifier," *Electron. Lett.*, vol. 33, no.10, pp. 879-880, May 1997.

[7] A.H.Gnauck, et al., "Transmission of two wavelength-multiplexed 10 Gbit/s channels over 560 km of dispersive fibre," *Electronics Letters*, vol. 30, no.9, pp.727-728, Apr 1994.

[8] S. Watanabe, M. Shirasaki, "Exact compensation for both chromatic dispersion and Kerr effect in a transmission fiber using optical phase conjugation", *J. Lightw. Technol.*, vol. 14, no. 2, pp. 243–248 Mar 1996.

[9] W. Forysiak, and N.J. Doran, "Conjugate solitons in amplified optical fibre transmission systems", *Electron. Lett.*, vol. 30, no.2, pp154-155, Jan 1994.

[10] D.D. Marcenac, et al., "40 Gbit/s transmission over 406 km of NDSF using mid-span spectral inversion by four-wave-mixing in a 2 mm long semiconductor optical amplifier", *Electron. Lett.*, vol. 33, no. 10, pp. 879-880, May 1997.

[11] D. McGhan, et al., "5120 km RZ-DPSK transmission over G652 fiber at 10 Gb/s with no optical dispersion compensation," in *Proc. Optical Fiber Communication Conference*, Anaheim, USA, 2005, paper PDP27.

[12] M. G. Taylor, "Coherent detection method using DSP for demodulation of signal and subsequent equalization of propagation impairments", *IEEE Photonics Technol. Lett.*, vol. 16, no. 2, pp. 674–676, Feb 2004.

[13] X. Chen, and W. Shieh, "Closed form expressions for nonlinear transmission performance of densley spaced coherent optical OFDM systems," *Optics Express*, vol.18, no. 18, pp.19039-19054, May 2010

[14] P. Poggiolini, "Modeling of non-linear propagation in uncompensated coherent systems," in *Proc. Optical Fiber Communications Conference*, Anaheim, USA, 2013, paper OTh3G1.l

[15] A.D. Ellis, J. Zhao, and D. Cotter, "Approaching the non-linear Shannon limit," *J. Lightw. Technol.*, vol. 28, no. 4, pp. 423-433 Feb 2010.

[16] G. Goldfarb, M. G. Taylor, and G. Li, "Experimental demonstration of fiber impairment compensation using the split-step finite-impulse-response filtering method," *IEEE Photonics Technol. Lett.,* vol. 20, no. 22, pp. 1887–1889, Nov 2008.

[17] G. Liga, et al., "On the performance of multichannel digital backpropagation in high-capacity long-haul optical transmission," *Optics Express*, vol.22, no. 24, pp. 30053-30062, Dec 2014.

[18] T. Yoshida, et al., "Spectrally-efficient dual phase-conjugate twin waves with orthogonally multiplexed quadrature pulse-shaped signals," in *Proc. Optical Fiber Communication Conference*, San Francisco, California, 2014, paper M3C.6.

[19] M. D. Pelusi, "Fiber looped phase conjugation of polarization multiplexed signals for pre-compensation of fiber nonlinearity effect," *Optics Express,* vol. 21, no.18, pp.21423-21432, Sep 2013.

[20] A. D. Ellis, et al., "Capacity limits of systems employing multiple optical phase conjugators," *Optics Express*, vol. 20, no. 16, pp.20381-20393, Aug 2015.

[21] K. Solis-Trapala, et al., "Transmission Optimized Impairment Mitigation by 12 Stage Phase Conjugation of WDM 24x48 Gb/s DP-QPSK Signals," in *Proc. Optical Fiber Communication Conference*, Los Angeles, California, 2015, paper Th3C.2.

[22] I. Sackey, et al., "Kerr Nonlinearity Mitigation: Mid-Link Spectral Inversion versus Digital Backpropagation in 5×28-GBd PDM 16-QAM Signal Transmission," *J. Lightw. Technol.*, vol. 33, no. 9, pp. 1821-1827, May 2015.

[23] I. Sackey, et al., "Kerr nonlinearity mitigation in 5 × 28-GBd PDM 16-QAM signal transmission over a dispersion-uncompensated link with backward-pumped distributed Raman amplification," *Optics Express*, vol.22, no.22, pp. 27381-27391, Nov 2014.

[24] K. Solis-Trapala, T. Inoue, and S. Namiki, "Nearly-ideal optical phase conjugation based nonlinear compensation system," in *Proc. Optical Fiber Communication Conference*, San Francisco, California, 2014, paper W3F.8.

[25] H. Hu, et al., "Fiber nonlinearity compensation of an 8-channel WDM PDM-QPSK signal using multiple phase conjugations," in *Proc. Optical Fiber Communication Conference,* San Francisco, California, 2014, paper M3C.2.

[26] S. Yoshima, et al., "Nonlinearity mitigation through optical phase conjugation in a deployed fibre link with full bandwidth utilization," in *Proc. European Conference on Optical Communications*, Valencia, Spain, 2015, paper We2.6.3.

[27] K. Solis-Trapala et al., "Doubled transmission reach for DP-64QAM signal over field-deployed legacy fiber systems enabled by MSSI," in *Proc. European Conference on Optical Communications*, Valencia, Spain, 2015, paper Mo.3.6.2.

[28] M.H. Shoreh, "Compensation of nonlinearity impairments in coherent optical OFDM systems using multiple optical phase conjugate modules," *J. Optical Commun. and Networking*, vol. 6, no. 6, pp.549-558, Jun 2014.

[29] M. Morshed, et al., "Experimental demonstration of dual polarization CO-OFDM using mid-span spectral inversion for nonlinearity compensation," *Optics Express*, vol. 22, no. 9, pp. 10455-10466, May 2014.

[30] L.B. Du, M.M. Morshed, and A.J. Lowery, "Fiber nonlinearity compensation for OFDM super-channels using optical phase conjugation," *Optics Express*, vol. 20, no. 18, pp. 19921-19927, Aug 2012.

[31] I. Phillips, et al.," Exceeding the nonlinear-Shannon limit using Raman laser based amplification and optical phase conjugation," in *Proc. Optical Fiber Communication Conference*, San Francisco, California, 2014, paper M3C1.

[32] A. D. Ellis, et al., "Enhanced superchannel transmission using phase conjugation," in *Proc. European Conference on Optical Communications*, Valencia, Spain, 2015, paper We.2.6.4.

[33] P. Johannisson, and E. Agrell, "Modelling of Nonlinear Signal Distortion in Fiber Optic Networks," *J. Lightw. Technol.*, vol. 32, no. 23, pp. 4544-4552, Dec 2014.

[34] E. Agrell, et al., "Capacity of a nonlinear optical channel with finite memory," *J. Lightw. Technol.*, vol. 32, no. 16, pp. 2862-2876, Aug 2014.

[35] P. Poggiolini, A. Carena, Y. Jiang, G. Bosco, V. Curri, F. Forghieri, "Impact of low-OSNR operation on the performance of advanced coherent optical transmission systems," in *European Conference on Optical Communications*, Cannes, France, 2014, paper Mo.4.3.2.

[36] J. Tang, "A comparison study of the Shannon channel capacity of various nonlinear optical fibers", *J. Lightw. Technol.*, vol.24, no.5, pp.2070-2075, May 2006.

[37] A.D. Ellis, et al., "The Impact of Phase Conjugation on the Nonlinear-Shannon Limit," in *Proc. Nonlinear Optical Signal Processing*, Nassau, The Bahamas, 2015, paper TuF3.2.

[38] G. Gao, X. Chen, and W. Shieh, "Influence of PMD on fiber nonlinearity compensation using digital back propagation", *Optics Express,* vol. 20, pp. 14406-14418, Jun 2012.

[39] M. Tan, et al., "Extended Reach of 116 Gb/s DP-QPSK Transmission using Random DFB Fiber Laser Based Raman Amplification and Bidirectional Second-order Pumping," in *Proc. Optical Fiber Communications*, Los Angeles, USA, 2015, paper W4E.1.

[40] G. Tzimpragos, et al., "A Survey on FEC Codes for 100G and Beyond Optical Networks, "*Communications Surveys & Tutorials,* DOI:10.1109/COMST.2014.2361754, Oct. 2014.

[41] M.F.C. Stephens, et al., "1.14Tb/s DP-QPSK WDM polarization-diverse optical phase conjugation," *Optics Express*, vol. 22, no.10, pp.11840-11848, May 2014 .

[42] R. Maher, et al., "Spectrally Shaped DP-16QAM Super-Channel Transmission with Multi-Channel Digital Back Propagation," *Scientific Reports*, vol. 5, pp.8214, Feb 2015.

[43] M. Tan, et al., "Evaluation of 100G DP-QPSK long-haul transmission performance using second order co-pumped Raman laser based amplification", *Optics Express*, vol. 23, pp 22181-22189, Aug 2015.